Original Article

High Performance Polymers

High Performance Polymers
1–14

DOI: 10.1177/0954008315585012
hip.sagepub.com

Effect of air plasma treatment on interfacial shear strength of carbon fiber–reinforced polyphenylene sulfide

Dongxia Xu[1], Baoying Liu[1], Gang Zhang[2], Shengru Long[2], Xiaojun Wang[2] and Jie Yang[2,3]

Abstract

Plasma treatment, an environmentally safe method, was applied for surface modification of carbon fibers (CFs) and polyphenylene sulfide (PPS) fibers. The morphology, crystallization property, thermal stability, and chemical properties of CF/PPS composites were determined, respectively, by scanning electron microscopy, differential scanning calorimetry, thermogravimetry analysis, and X-ray photoelectron spectroscopy. Interfacial micromechanical performance of CF/PPS composites was investigated by microbond test. The influence of plasma treatment on the apparent interfacial shear strength (τ_{app}) of CF/PPS micro-composite was systematically evaluated. The plasma treatment of CF reduced the τ_{app} of the micro-composite by 13.7% and that of CFs and PPS fibers by 3.4%. However, the plasma-treated PPS fibers increased the τ_{app} of the micro-composite by 17.1%. The present study demonstrates that matching of polarity between CF and the resin plays a great role in reinforcement of interfacial property.

Keywords

Air plasma treatment, polyphenylene sulfide, carbon fiber, microbond test, interfacial shear strength

Introduction

The attractive, semicrystalline engineering thermoplastic, polyphenylene sulfide (PPS) is widely used for defense and military purposes by virtue of its outstanding thermal stability, excellent chemical resistance, inherent flame resistance, and so on.[1,2] However, its rather low impact toughness and tensile strength constrain its applications.[3,4] In addition, with recent advances in science and technology, the traditional single material is no longer expected to meet the needs of diverse applications. Fortunately, there are many polymer composites, which are versatile enough to improve the properties of PPS fibers.[5]Among these, carbon fiber (CF)-reinforced polymer composite has been widely used by virtue of its good mechanical behavior, high strength to weight ratio, light weight, and so on.[6,7] The CFs can overcome the disadvantages of PPS and enable the composites to be widely used in the fields of transport, manufacture, aerospace engineering, sports equipment, and civil constructions.

The comprehensive properties of fiber-reinforced composites depend on the intrinsic property of the fibers (or resin matrix), the volume fraction of fibers (or resin matrix) and their interphases. The interphase is now considered a distinct, three-dimensional phase surrounding the reinforcing phase.[8] It is widely realized that the interface between the fiber and the matrix plays an important role in transmitting applied load from the matrix to the reinforced fiber. The transmission of applied load controls the overall mechanical behavior of the composites, such as the off-axis strength and fracture toughness and so on. The processing conditions of the composites have a dominant effect on the interfacial character and ultimately on the properties of the composites.[9]

The main disadvantage of the CFs is its chemical inertness, which usually leads to its poor compatibility with the matrix.[10] Besides this limitation, the polymers do not

[1] College of Polymer Science and Engineering, Sichuan University, Chengdu, China
[2] Institute of Materials Science and Technology, Sichuan University, Chengdu, China
[3] State Key Laboratory of Polymer Materials Engineering, Sichuan University, Chengdu, China

Corresponding author:
Jie Yang, State Key Laboratory of Polymer Materials Engineering, Sichuan University, Chengdu 610065, China.
Email: ppsf@scu.edu.cn; yangjie_scu@163.com

provide adequate adhesion bonding interaction because of their hydrophobic nature and relatively low surface energy.[11] Therefore, the mechanical property of the interphase is commonly the weakest part of the composites because of poor interfacial bonding.[12] Research in interface modification of CF-reinforced resin composites thus becomes an important prerequisite to developing the composites' applications. Two major approaches are available for enhancing the interphase of CF-reinforced resin composites: (i) modification of polymer matrix[13] and (ii) surface treatment of CFs. The second approach can be adopted in many ways, including electrochemical oxidation, liquid phase chemical oxidation, fiber sizing and coating, and high-energy beam irradiation.[14–18] Resin matrix modification, however, usually involves chemical synthesis, which is less efficient and expensive. Compared to modification of polymer matrix, high-energy beam irradiation, such as plasma treatment, is more efficient and inexpensive. Yao et al. reported that sizing agent can improve the interfacial adhesion of the composites.[19] CF sizing agent can be mainly a solution or an emulsion.[20] Solution sizing agents are organic solutions, such as polyvinyl alcohol, epoxy resin, or polyurethane resin. The structure of these sizing agents is similar to that of the matrix resin, which can effectively improve the compatibility between resins and CFs. Emulsion sizing agent can be made by using a resin as the main component and an additive, such as polyurethane resin, epoxy resin, and composite resin. Emulsion sizing agent containing the surfactants can effectively improve the surface wettability of CF. The desized CFs have lower concentration of activated carbon atoms and lower polar surface energy.[19] The compatibility between composite components can be enhanced mostly by either physical or chemical interfacial modifications.[21,22] Compared with the chemical treatment, the physical surface treatment is environmentally more friendly and more efficient with more popular application prospects. A great deal of interest has been generated on plasma treatment, which offers stable and long-lasting surface energy enhancement.[23] It not only induces physical and chemical changes between the CF and the polymer matrix but also retains the original performance of the materials. Moreover, the processing is clean and efficient.[24] There is timeliness in the plasma treatment,[25,26] where plasma-treated specimens will lose their efficacy after a period of time. Conventional plasma treatment requires low pressure, and hence, the specimens must be processed in a vacuum chamber. To overcome this constraint, atmospheric pressure plasma has been developed. The operating conditions of near ambient temperature and atmospheric pressure eliminate the need for expensive vacuum systems. Till now, most researchers have been emphasizing on plasma treatment of thermosetting resin composites reinforced with CFs.[10] However, the effect of plasma treatment on the properties of CF/PPS composites and the extent to which it can improve the interfacial adhesion of the composites are unclear.

The properties of fiber-reinforced composites are generally evaluated by means of various conventional tensile, flexural, and fatigue tests. Although these tests provide valuable information about the macroscopic properties of the composites, they fail to provide information on pure interfacial shear strength (IFSS; τ_{app}) between the fiber and the matrix. Besides these results are strongly dependent on other factors, such as specimen geometry, fiber/matrix volume ratio, and fiber property. Overcoming the weaknesses of traditional macroscopic methods, various tests, such as fragmentation test,[27] pushout test,[28] pull-out test,[29] and microbond test,[30] enables the measurement of the fiber–matrix IFSS (τ_{app}) on microscopic scale. In these tests, shear force is applied to the interface, consequent to which interfacial debonding occurs. The IFSS is then calculated based on the ultimate shear load and the debonding area. Among the above-mentioned tests, the microbond test is favored more because of its good discrepancy in results, repeatability, and easy maneuverability.

For this research, the interfacial adhesion behavior of PPS/CF composites was systematically studied. Air dielectric barrier discharge (DBD) plasma treatment was applied to modify the PPS/CF interface. The effect of plasma treatment on the properties of CFs and the timeliness were also studied. The objective of this study is to elucidate the mechanism of plasma treatment on the interfaces between CFs and PPS resins.

Experimental method

Materials

Carbon fibers. Commercial T700-grade high-strength CFs (T700SC-12000, Toray Co., Ltd, diameter of 7 mm) were used in this study because their strain rate is insensitive over a wide range of loading rates.[31] Besides, they are also widely utilized as reinforcing components in composite structures. The fibers were processed with sizing agents but without any sizing extractions.

Matrix. PPS resin, fiber grade, was supplied by Deyang Chemical Co., Ltd (Chengdu, China) with glass transition temperature (T_g) and melting temperature (T_m) of around 95°C and 285°C, respectively.

Sample preparation

Preparation of surface-modified CFs and PPS fibers. DBD plasma treatment apparatus was used in this study to modify the surface of CFs and PPS fibers. The working procedure, illustrated in Figure 1, was taken from a previous report.[32] A gap barrier of narrow dimension exists between two metal plate electrodes. The bottom-side electrode was grounded, while the upside electrode, covered with alumina, was connected to a power supply, which was providing high

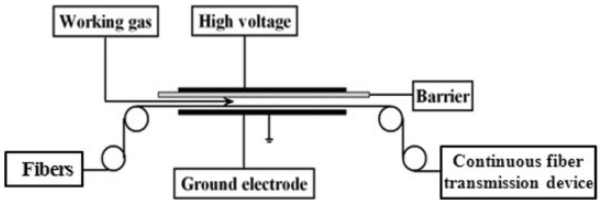

Figure 1. Schematic apparatus of DBD plasma. DBD: dielectric barrier discharge.

alternating current voltage continuously. Thus, the discharge could be produced between two electrodes during the process. The power supplied was kept at 300–2000 W.

CFs and PPS fibers were treated by passing them through the discharge area. CFs were treated by different discharge power densities (F) of 0.3, 0.5, 0.8, 1.0, 1.3, and 1.5 kW cm^{-3} for 60 s, respectively. In addition, they were also treated for different treatment times (t) of 5, 20, 60, 120, and 200 s at the discharge power density of 1.0 kW cm^{-3}. PPS fibers were treated at 1.0 kW cm^{-3} for 30 s.

Preparation of CF/PPS microdroplet. A novel, simple, and efficient procedure has been established for preparing thermoplastic composite microdroplets (see Figure 2).[33] Pure PPS resin was melted, pulled into fibers, and then the fibers were knotted slightly around the CF. The sample was then melted at 320°C. The specimen was retained in the molten state until it fully formed a testable droplet and then cooled down to ambient temperature. Finally, the sample was annealed at 120°C for 12 h.

Microbond test. The IFSS (τ_{app}) was investigated using the microbond test. The fiber was pulled out when the shearing force exceeded the interfacial bond strength, and the force was continuously recorded during the experiment by a load cell. The maximum pull-out force was obtained from the load–displacement curve of each test. The corresponding fiber diameter and embedded length were measured using the optical microscope equipped with a high-resolution color charge-coupled device camera (EC3001) and Studio Measure software (EC image). The τ_{app} could be calculated using equation (1),[34] given below, which is traditionally used to estimate the surface modification efficiency of the matrix and/or the fiber:

$$\tau_{app} = \frac{F_{max}}{\pi d_f l_e}, \quad (1)$$

where d_f is the fiber diameter, l_e is the embedded length, and F_{max} is the maximum pull-out force. More than 30 equal measurements were conducted to obtain the average τ_{app} value. The test speed of microbond tests was set to 0.02 mm s^{-1}, as suggested by our previous research.[33]

Characterizations

Scanning electron microscopy

The surface morphology of CFs and specimens, before and after the microbond test, was studied by a JEOL JSM-7500 scanning electron microscopy (SEM; Japan), working at an acceleration voltage of 20 kV. All the samples were sputtered with a 10 nm layer of gold prior to examination under SEM.

Monofilament strength test

Monofilament strength of CFs, before and after plasma treatment, was measured by a single-fiber electronic tensile strength tester (YG001A, Tai Cang Textile Factory, China) working at a tensile rate of 10 mm min^{-1}. The upper and lower clamping pressures were set in the range of 0.2–0.3 MPa.

X-Ray photoelectron spectra

Surface chemical composition of the plasma-treated PPS fibers and CFs was measured using X-ray photoelectron spectroscopy (XPS; XSAM800, Kratos Company, England) with a magnesium K_α X-ray source. The scan spectrum was obtained over a range of 0–1100 eV.

Water contact angles

Water contact angles on the PPS film surfaces were measured according to a sessile drop method at 25°C in1 h after plasma treatment using a contact angle meter (DSA 100, Krüss, Hamburg, Germany).[35] The average contact angle, from five measurements, was determined with a standard deviation of 2–3°C.

Thermogravimetric analysis

Thermal stability experiments were performed using a thermogravimetric analyzer (TGA Q500, TA Instruments, New Castle, Delaware, USA). The samples were placed in a 70.0-μL of alumina pan and heated at a rate of 10°C min^{-1} from 50°C to 800°C under nitrogen (N_2) flow.

Differential scanning calorimetry

The crystallization and melting properties of the composites were studied using a differential scanning calorimetry analyzer (DSC 204F1, Netzsch Instruments, Germany). The samples were first heated at the rate of 10°C min^{-1} from 40°C to 320°C and then that temperature was maintained for 4 min to eliminate thermal history. The samples were then cooled to 40°C at the rate of 10°C min^{-1} and then maintained at 40°C for 2 min. Finally, all the samples were secondarily heated up to 320°C following the same procedure. All procedures were carried out under N_2 flow

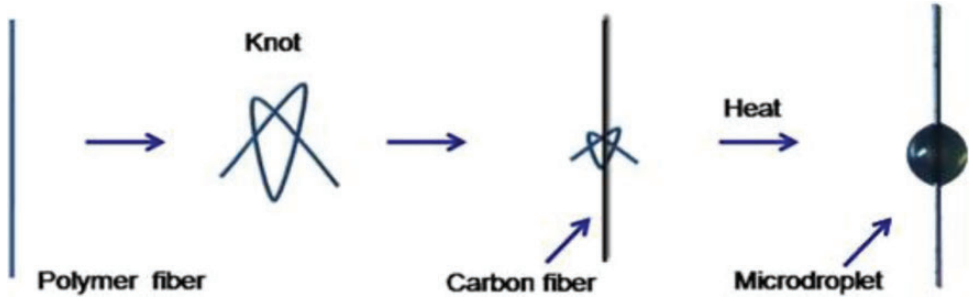

Figure 2. Forming procedure of thermoplastic resin droplets on a single CF and an optical microscope photograph of microdroplets. CF: carbon fiber.

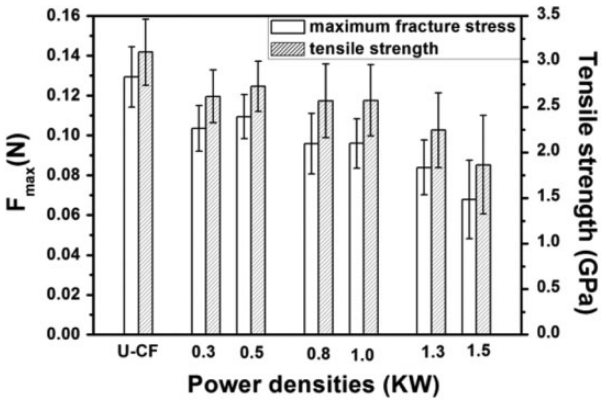

Figure 3. Influence of discharge power density on the tensile strength of CF monofilament (discharge time: 60 s). CF: carbon fiber.

at a flow rate of 50 mL min^{-1}. From the DSC curve, the crystallinity of PPS in the composite was calculated using the following equation:

$$X_c(\%) = \frac{\Delta H_m}{(\Delta H_0 \times \omega)} \times 100, \quad (2)$$

where X_c denotes the crystallinity of PPS in the composite, ΔH_m the heat of crystallization absorbed by 1 g of crystallizing melt, ΔH_0 is the heat of melting of a perfectly pure PPS crystal, and ω is the mass friction of pure PPS in the composite.

Results and discussion

Influence of air plasma treatment on CFs

Morphological study and monofilament strength test. The monofilament strength of CFs was evaluated by a monofilament strength tester. It can be seen from Figure 3 that the monofilament strength decreased slightly when the discharge power density was less than 1.0 kW cm^{-3} and it fell by only 9.2% when the discharge power density was 1.0 kW cm^{-3}. Obviously, the monofilament strength declined with increase in the discharge power density beyond 1.0 kW cm^{-3}. Therefore, the discharge power density was controlled at 1.0 kW cm^{-3} for the present study.

The SEM images of CF surfaces, before and after plasma treatment, at 1.0 kW cm^{-3} for different time durations, are shown in Figure 4. A very clean and smooth surface appeared on the untreated CF (CF-0). However, some spots appeared on the fiber surface after plasma treatment for 5 s, and a few streak flaws after treatment for 10 s. After increasing the treatment time to 60 s, many protrusions appeared on the CF surface. Overall, it was found that the surfaces of CF-120 and CF-200 were much cleaner and smoother than those of other samples when the plasma treatment was increased to 120 s and 200 s. This obviously suggests that the CF was significantly etched after air DBD plasma treatment for 60 s, possibly because of the surface etching effects and oxidative reactions of plasma treatment. Incidentally, it was found that the sizing layer, coated on the CFs surface, could be removed to some extent.

It thus follows that air DBD plasma treatment on CFs for 60 s, with 1 kW cm^{-3} of discharge voltage and a slight decrease in monofilament strength, could change the surface topography of CF, enhance the surface roughness, and provide a larger surface area than what is possible by other treatment methods. The increased roughness of fiber surface is beneficial to micromechanical interlocking, which is an important factor in determining interfacial adhesion.[36] So, CF with plasma treatment at 1 kW cm^{-3} for 60 s was applied during subsequent research.

XPS analysis. XPS was applied to analyze the chemical changes that occur in CFs after plasma treatment. Figure 5 shows a general survey of the surface atomic distribution of the main elements for original and plasma-treated samples. As can be seen in Table 1, the O/C atomic ratio increased after air plasma treatment of the sample, implying thereby that the fiber surface was modified significantly. More information could be obtained by deconvolution of C1 peaks. Figure 6 shows the C1s spectra of the original and plasma-treated CFs with different timelines. The most significant difference between the two is the increase in the intensities of –COOH and –COOR peaks. These changes correspond to anincrease in the O/C atomic ratio, reported

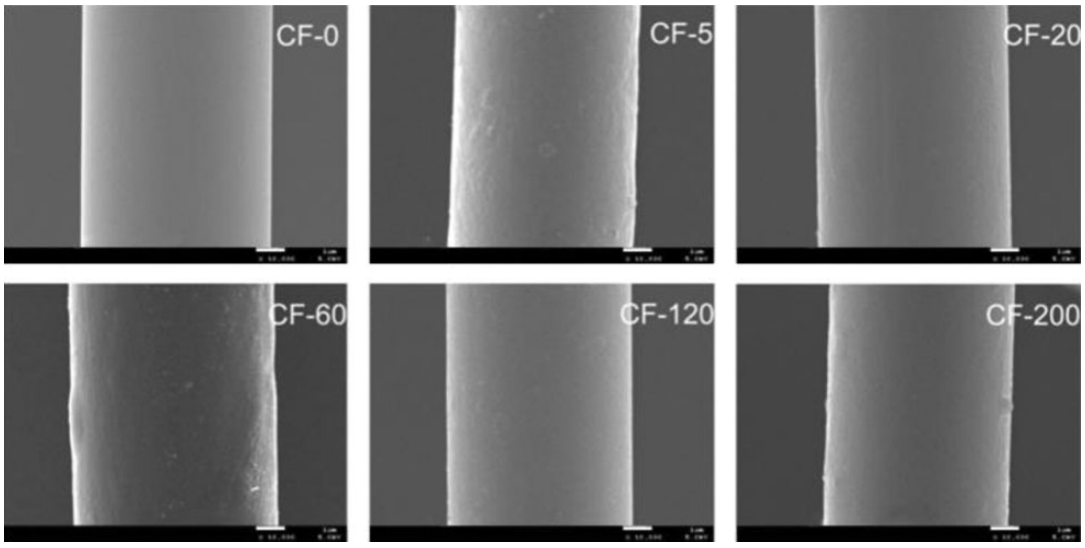

Figure 4. SEM images of CF with air plasma treated under 1.0 kW with different processing time. SEM: scanning electron microscopy; CF: carbon fiber.

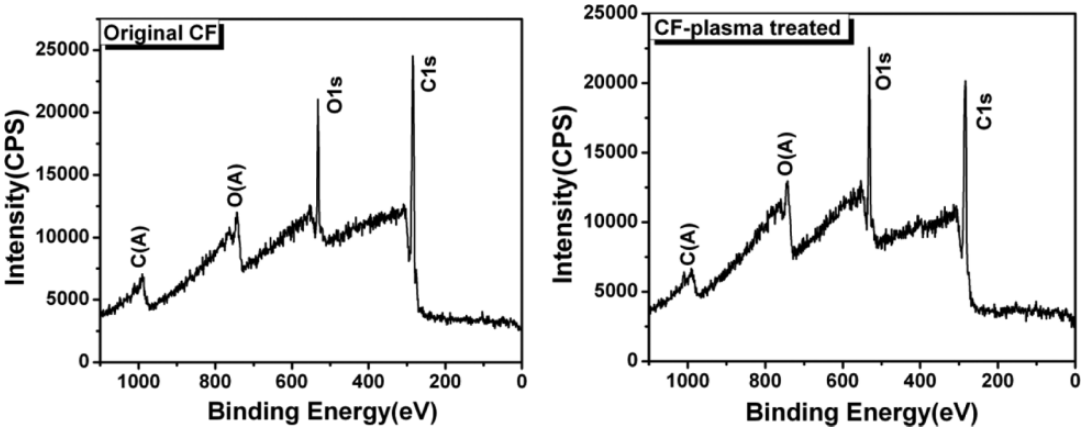

Figure 5. XPS survey spectra of CF surfaces with and without plasma treatment. XPS: X-ray photoelectron spectroscopy; CF: carbon fiber.

in Table 1, after plasma treatment of the sample. The significant increase in surface oxygen content may lead to high chemical activity of the fibers.

With passage of time after plasma treatment, the reactive groups on the surface of the material may decline or undergo deoxidation.[25,26] Table 1 shows the concentration of O and C elements on CFs surface, after air plasma treatment at 1 kW cm^{-3} for 60 s over different time period, say 0.8, 6, 24, 72, and 168 h. It can be seen that the O/C atomic ratios remained almost stable even after increasing the treatment time. However, the deconvolution of C1s peaks seen in Figure 6 and Table 2 indicate that the concentration of –COOH and –COOR declined but that of –C=O increased within 3 days. The percentages of polar groups on the surface of CFs decreased dramatically after a week, whereas those of C–H and C–C increased, compared with the corresponding percentages of untreated samples. All these results can be explained as due to the removal of sizing agent and the grafting of active groups onto the surface of the CFs. Besides, the active groups lost their activity

Table 1. Timeliness of the elements concentration on CF surface with air plasma treatment. CF: carbon fiber.

	Elemental composition		Composition ratio
Time (h)	C (%)	O (%)	O/C
0	83.2	16.8	20.2
0.8	74.9	25.1	33.5
6	77.8	22.2	28.5
24	75.7	24.3	32.1
72	75.4	24.6	32.6
168	77.4	22.6	29.2

O: oxygen; C: carbon.

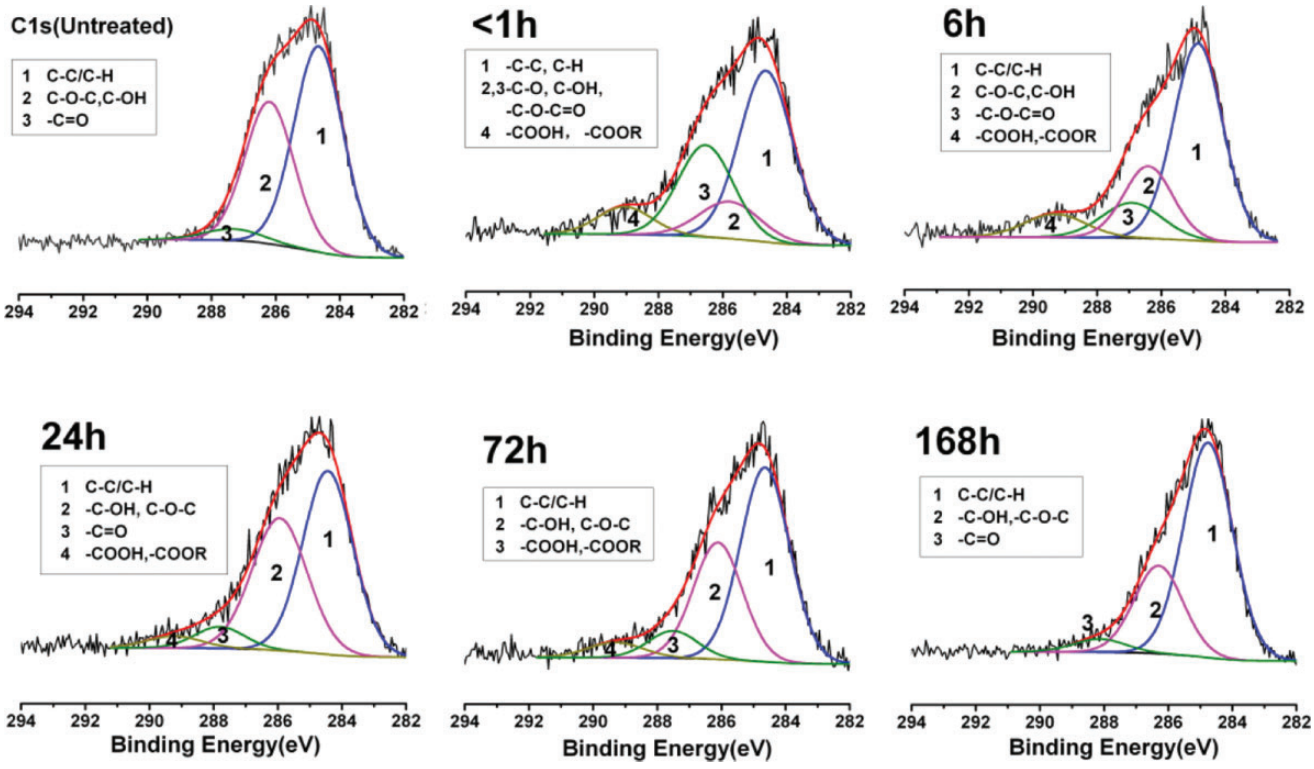

Figure 6. Timeliness of C1s spectra of CFs with plasma treatment. CF: carbon fiber.

Table 2. Timeliness of contents of carbon functional groups by C1s XPS.

	Carbon-containing groups (%)			
Time (h)	284.8 (eV) C–C, C–H	285.8–286.9 (eV) C–O–C, C–OH, C–O–C=O	287.7 (eV) –C=O	289.3 (eV) –COOH, COOR
0	56.9	39.3	3.8	—
0.8	50.8	40.8	—	8.4
6	57.8	33.7	—	8.5
24	50.5	40.2	5.8	3.5
72	54.7	32.9	7.6	4.8
168	67.9	27.7	4.4	—

XPS: X-ray photoelectron spectroscopy.

because of absorption of moisture and impurities. Yet the surface of CFs could still retain a great amount of active groups up to 6 h after plasma treatment.

From the foregoing analysis, it thus emerged that all subsequent experiment samples with plasma treatment should be prepared within 6 h to sustain their activity.

Interfacial adhesion. Typical plots of the maximum pull-out force as a function of embedded length for microbond specimens of untreated and plasma-treated CF/PPS are shown in Figure 7. The plots show that F_{max} increased almost linearly with increasing l_e. The plots of individual τ_{app} versus l_e, according to equation (1), are shown in Figure 7. The measured τ_{app} remained almost the same with increasing l_e value, suggesting that τ_{app} is not related to l_e. However, the average value of τ_{app} could be calculated, based on the individual τ_{app} of each droplet. The values of τ_{app} of PPS/CF samples, with/without plasma-treated CF, are shown in Table 3. According to the statistical results shown in Table 3, the value of τ_{app} of the specimens with plasma-treated CFs is lower than that of the specimens with CFs not subjected to plasma treatment. It is well known that the molecular chain of PPS is nonpolar; however, the CFs with plasma treatment obtained higher chemical activity than that were not subjected to plasma treatment. This leads to an unmatched polarity between the interface of PPS resin and CFs. Moreover, the size layer coated on the surface of CFs, which is considered beneficial to interfacial adhesion,[18] was removed to some extent. As a result, the interfacial interaction of plasma-treated CFs-reinforced PPS composites became weaker than that of the pristine composite samples.

Influence of air plasma treatment on PPS fibers

The surface properties of PPS fibers were obviously influenced by increase in discharge power density and treatment time. Nevertheless, PPS fibers could be easily scorched and carbonized by applying high discharge power density for

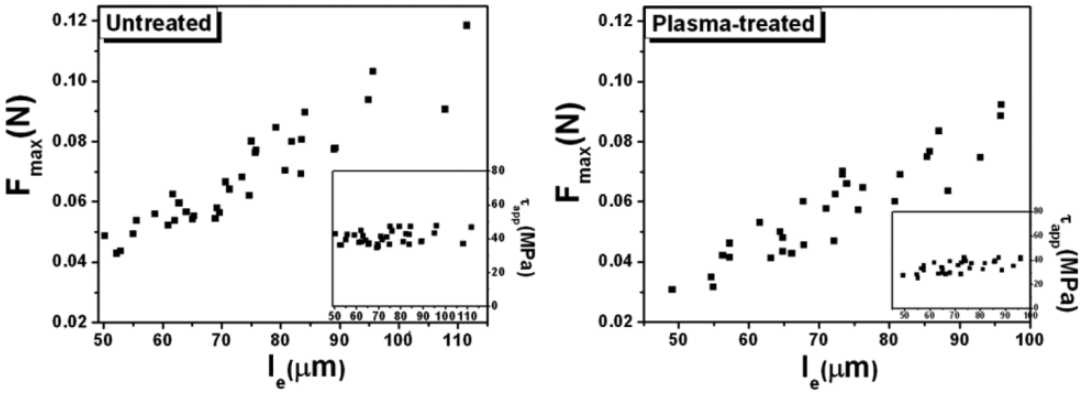

Figure 7. Microbond test results of CF/PPS composites with/without plasma-treated CF. CF: carbon fiber; PPS: polyphenylene sulfide.

Table 3. Interfacial shear strengths of PPS/CF samples with plasma-treated CF and untreated CF.

Interfacial shear strength	Not plasma treated	Plasma treated
τ_{app} (MPa, SD)	40.9 ± 3.9	35.3 ± 5.0

CF: carbon fiber; PPS: polyphenylene sulfide; SD: standard deviation.

a long time. PPS fibers with plasma treatment under 1 kW cm^{-3} for 30 s were applied in subsequent research.

XPS analysis

The introduction of oxygen-containing groups into plasma-treated polymers was the main reason for the increase of surface free energy. To study the difference between the surface chemical compositions of plasma-treated and untreated PPS fibers, XPS was used. The survey spectra revealed that carbon (C1s), oxygen (O1s), and sulfur (S2p) were the inherent elements. After plasma treatment, a new element, corresponding to nitrogen (N1s), emerged, and the O/C atomic ratio increased as shown in Figure 8. Deconvolution of different elements was conducted to compare the changes in the functional groups. Particularly, deconvolution of C1s, N1s,[37] and S2p[32] peaks could give more information. The C1s spectrum of the untreated and plasma-treated surface could be decomposed into three components: a component at 284.8 eV due to the C–C bonds, a component at 285.8 eV due to C–O bonds, and a component at 288.5 eV due to the O–C=O and O–C=NH bonds as shown in Figure 9. Figure 10 shows the N1s spectra of the PPS surfaces after plasma treatment. It was found that –NN– and $–NN_2–$ bonds appeared at 401.8 eV and 399.8 eV because of absorption of free nitrogen atoms from plasma air. The S2p spectrum of the untreated and plasma-treated samples could be decomposed into two components, as shown in Figure 11, a component at 165.6 eV due to sulfoxide (S=O) and a component at 168.9 eV due to sulfone (O=S=O). Both of them were oxidized from nonpolar thioether bonds. The contents of functional groups on the surface of PPS fibers, before and after plasma treatment, are shown in Table 4.

The foregoing plasma treatment results reveal strong oxidation level on the surface of PPS fibers. On exposure of the PPS fibers to air plasma, the molecules on the fiber surface were subjected to a high reactive regime of DBD, which could generate a wide range of active substances, including atomic oxygen, ozone, nitrogen oxides, neutral molecules, radicals, and ultraviolet radiation. The main reactive substance responsible for oxygen-containing material was oxygen atom formed in the discharge because of the dissociation of molecules of O_2 by the electron impact. After the plasma treatment, PPS surface was thus polar and active.

Wettability analysis

Contact angle results are shown in Figure 12. The water contact angles of samples of air plasma-treated PPS films decreased significantly, in comparison with those of the untreated samples, indicating that the surface free energy increased. Also, it decreased with increase in the treatment time. These results are consistent with those obtained from XPS analysis.

Thermal stability and crystallization performance analysis

The thermal stability and crystal structure of PPS may be influenced by high temperature and oxygen.[38,39] Thermal stability was studied by analyzing the degradation reaction of the samples, after subjecting them to TGA. A comparison of the thermal stabilities of PPS, before and after the plasma treatment, is shown in Figure 13, and the characteristic parameters are presented in Table 5. The thermal stability of plasma-treated PPS improved consequent to the introduction of sulfone groups, whose thermal stability is better than that of sulfide bonds.[40]

Also, DSC was applied to determine the crystallization property of PPS fibers. The representative DSC curves of

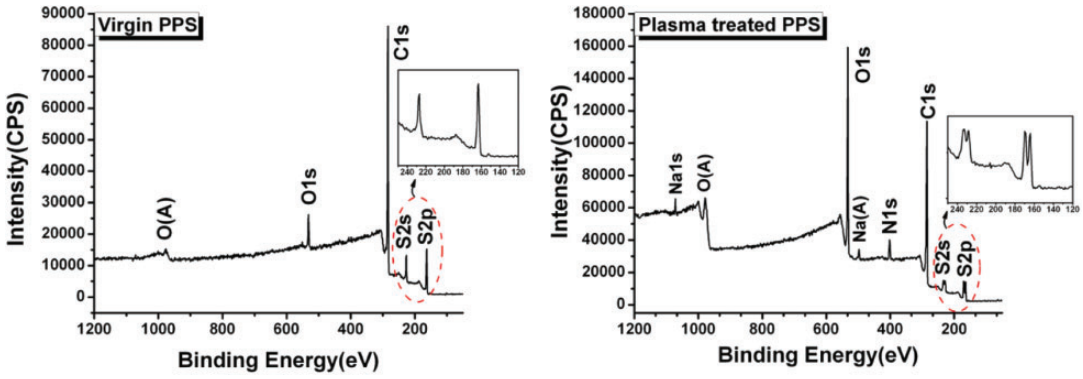

Figure 8. XPS survey spectra of PPS fiber surfaces with and without plasma treatment. XPS: X-ray photoelectron spectroscopy; PPS: polyphenylene sulfide.

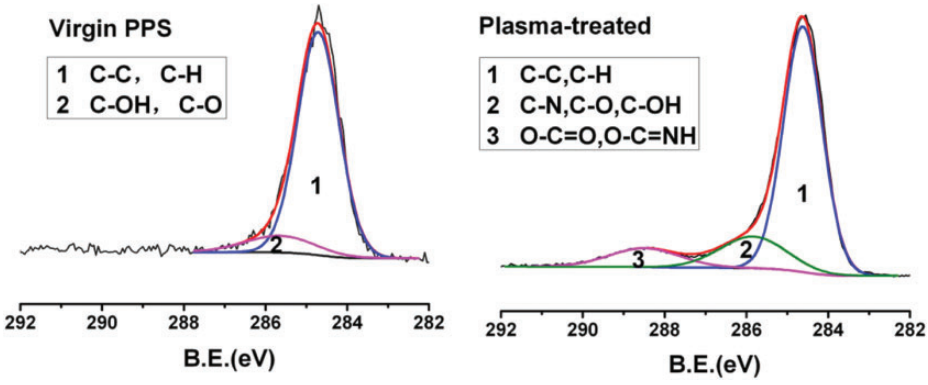

Figure 9. C1s spectra of PPS before and after plasma treatment. PPS: polyphenylene sulfide.

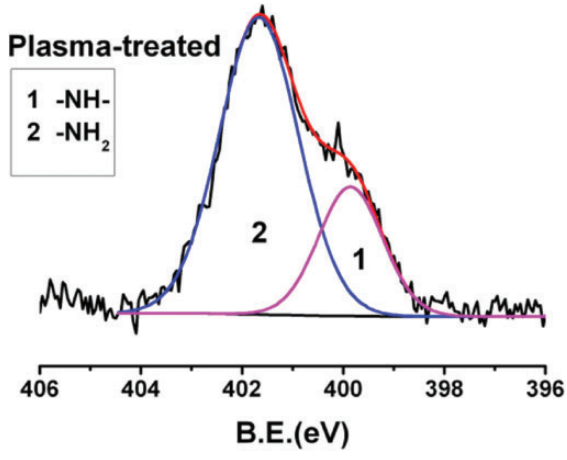

Figure 10. N1s spectra of PPS after plasma treatment. PPS: polyphenylene sulfide.

PPS fibers, before and after plasma treatment, are shown in Figure. 14, and the characteristic parameters are summarized in Table 6. The crystallization peak of plasma-treated PPS resin shifted to a lower temperature, besides becoming wider. These changes indicate that the introduction of a small amount of polar groups would hinder the movement of PPS molecular chains, facilitating thereby larger supercooling required for PPS crystallization. Nevertheless, plasma treatment could not significantly affect either crystallinity or melting temperature of PPS resin because the amount of polar groups, introduced by polar treatment on fibers surface, was too small to change the molecular structure of the resin under the surface.

To sum up, the plasma treatment showed little effect on thermal stability and crystallinity of the resin.

Morphology analysis of the microbond samples

The SEM images of microbond specimens, before and after debonding, are shown in Figure 15. Prior to microbond test, there is little difference in morphology between plasma-treated and untreated samples (see Figures 15(a) and (b)). But, after microbond test, the CF surface of the untreated sample was smoother with a little resin attached after debonding. Obviously, the matrix was detached from the fiber surface of the pristine samples, as shown in Figure 15(a). Nevertheless, much more residue of matrix was attached to the surface of CF in the plasma-treated sample, as shown in Figure 15(b), implying that plasma treatment had an obvious influence on the interfacial property of CF/PPS composite. The foregoing observations further suggest that the interfacial adhesion

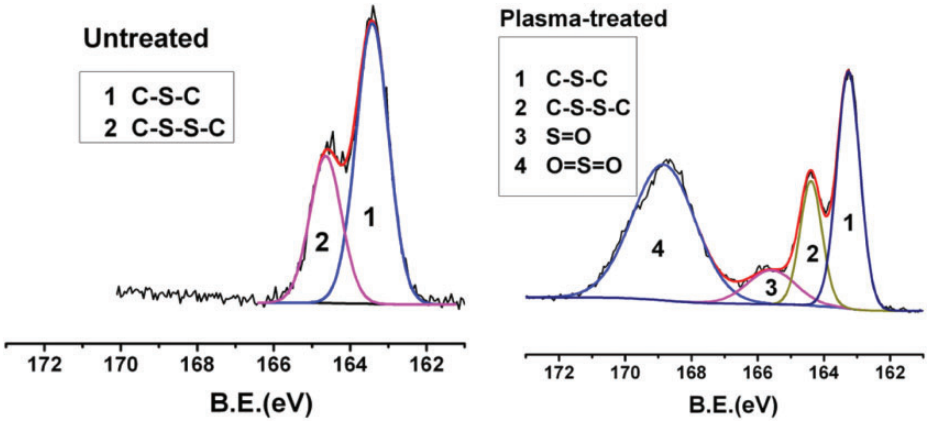

Figure 11. S2p spectra of PPS before and after plasma treatment. PPS: polyphenylene sulfide.

Table 4. Contents of functional groups on the surface of PPS fibers, before and after the plasma treatment.

	Carbon-containing groups (%)			Sulfur-containing groups (%)		
PPS	284.8 (eV) C–C, C–H	285.8 (eV) C–N, C–OH, C–O–C	288.5 (eV) O–C=O O–C=NH	163.3–164.5 (eV) C–S–C, C–S–S–C	165.6 (eV) S=O	168.9 (eV) O=S=O
Untreated	88.8	11.2	—	100	—	—
Plasma treated	73.8	16.1	10.1	44.7	8.9	46.4

PPS: polyphenylene sulfide.

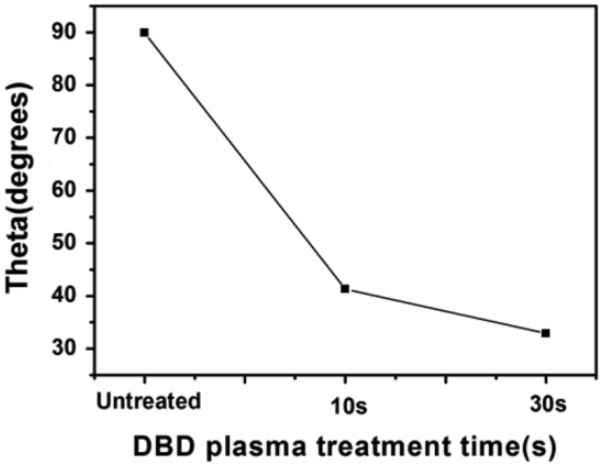

Figure 12. Contact angle of water of PPS films under different DBD plasma treatment times (1.0 kW cm^{-3}). PPS: polyphenylene sulfide; DBD: dielectric barrier discharge.

between PPS and CFs is stronger after plasma treatment on PPS fibers than before tratment.

Interfacial adhesion

For final results, subsequent microbond test was conducted as previously stated. Plots of the maximum pull-out force and individual τ_{app}, as a function of l_e for microbond

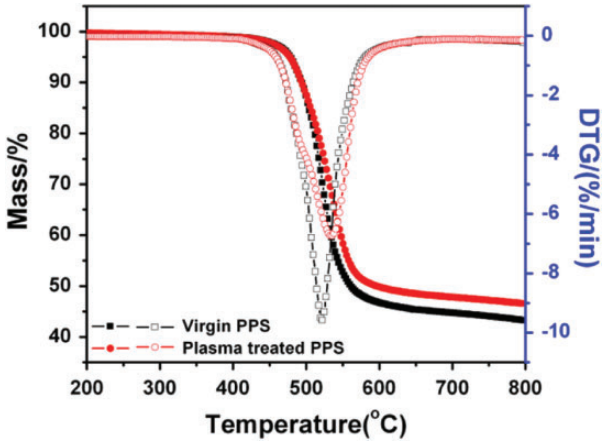

Figure 13. Comparison of thermal stability of PPS before and after plasma treatment. PPS: polyphenylene sulfide.

Table 5. TGA characteristic parameters of PPS, before and after plasma treatment.

Samples	$T_{5\%}$ (°C)	T_{max} (°C)	Weight loss at 800°C (%)
Untreated PPS	471.3	521.5	56.8
Plasma-treated PPS	478.1	534.5	53.5

TGA: thermogravimetric analysis; $T_{5\%}$: 5% weight loss temperature; T_{max}: maximal degradation temperature; PPS: polyphenylene sulfide.

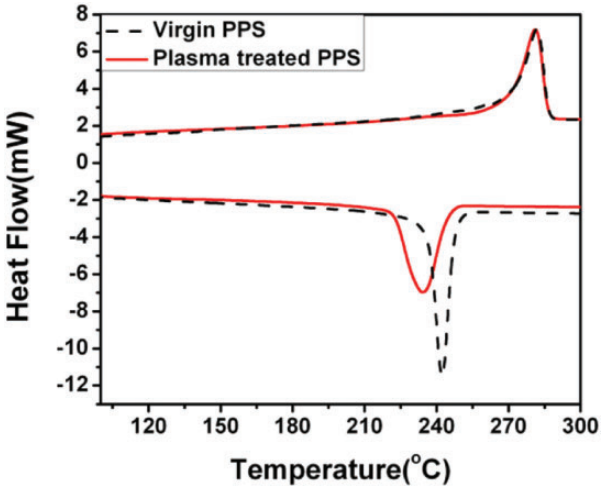

Figure 14. DSC non-isothermal crystallization curves (down) and the following melting curves (up) of PPS with and without plasma treatment. DSC: differential scanning calorimetry; PPS: polyphenylene sulfide.

Table 6. DSC characteristic parameters of PPS, before and after plasma treatment.

Samples	T_c (°C)	ΔH_m (J g^{-1})	T_m (°C)	X_c (%)
Untreated PPS	342.3	40.4	281.8	52.8
Plasma treated PPS	234.2	37.9	281.2	49.6

DSC: differential scanning calorimetry; PPS: polyphenylene sulfide; T_c: crystalline temperature; ΔH_m: heat of crystallization absorbed by 1 g of crystallizing melt; T_m: melting temperature; X_c: degree of crystallinity.

specimens of plasma-treated and untreated CF/PPS, are shown in Figure 16. These plots show that F_{max} increased almost linearly with increasing l_e and that the τ_{app} is not related to l_e. The average values of τ_{app} and corresponding standard deviations are shown in Table 7. In fact, the τ_{app} of the specimen, after plasma treatment on PPS fibers, is higher than that of the specimens not subjected to plasma treatment. The plasma treatment resulted in enhancement (17.1%) of the τ_{app} of the PPS fibers.

The interfacial adhesion achieved between PPS and CFs is stronger because of the presence of the polarized PPS molecular structure that can generate polar function groups, such as sulfone O=S=O, sulfoxide S=O, and O–C=O. These groups contribute to promoting cohesion by way of inducing chemical reactions or generating hydrogen bond with some components of the sizing agents on CFs. The interfacial reaction between the CF and plasma-treated PPS fiber is illustrated in Figure 17.

Influence of simultaneous air plasma treatment on CFs and PPS fibers

Both PPS fiber and CF can be grafted by active functional groups after plasma treatment. It is possible to achieve synergistic effect for enhancing CF/PPS interfacial adhesion by simultaneous plasma treatment of PPS fiber and CFs. The τ_{app} of CF/PPS composite was measured by microbond test after plasma treatment of both PPS fiber (1 kW cm^{-3} for 30 s) and CF (1 kW cm^{-3} for 60 s). Plots of the maximum pull-out force versus individual τ_{app}, as a function of l_e for microbond specimen of CF/PPS, are shown in Figure 18. The values of τ_{app} of CF/PPS composites, with plasma-treated CF, PPS, and CF/PPS composite, are shown in Figure 19. The average values of τ_{app} and corresponding standard deviations are shown in Table 8. From this Table, it can be seen that the τ_{app} of coprocessed specimens is lower than that of either the untreated specimen or the plasma-treated PPS fiber. Although the polar functional groups increased, the removal of sizing agent, which is beneficial to the interfacial bonding between the CF and PPS,[19] coated onto the surface of CFs by the plasma etch is the main reason for the decrease of τ_{app}.

Conclusions

In this article, the effect of DBD air plasma treatment on τ_{app} of CF-reinforced PPS was studied. The mechanism of plasma treatment on CF/PPS composites was discussed as well. The main conclusions drawn from this study are as follows:

1. Air plasma treatment led to distinct increase of specific surface area and roughness of CF surface. The size layer coated on the surface of CF was also removed to some extent. Besides, there was obvious increase in atomic ratios of O/C and the proportions of some reactive oxygen groups such as ester. All these changes resulted in increasing the specific surface area and the surface wettability. When air DBD plasma treatment time (t) was sustained for 60 s and the discharge voltage maintained at 1.0 kW cm^{-3}, the CFs underwent obvious changes in surface topography and chemical composition. The timeliness of plasma treatment can maintain for about 6 h.
2. The τ_{app} of the specimen decreased by about 13.7% after plasma treatment on CFs. The increased toughness could generate good micromechanical interlocking between the CFs and PPS fibers. As the PPS is a nonpolar thermoplastic polymer with an orderly arrangement of alternating phenylene and sulfide atoms, there can be little chemical bonding between the matrix and CF with reactive groups after plasma treatment, and this leads to the decrease of τ_{app}. The nonpolarity of PPS molecular structure is responsible for poor interfacial adhesion between the CF and PPS. Another reason for the decrease of τ_{app} is part removal, by plasma etching, of the sizing agent coated on the surface of CF, which is beneficial to the interfacial bonding between CF and PPS.

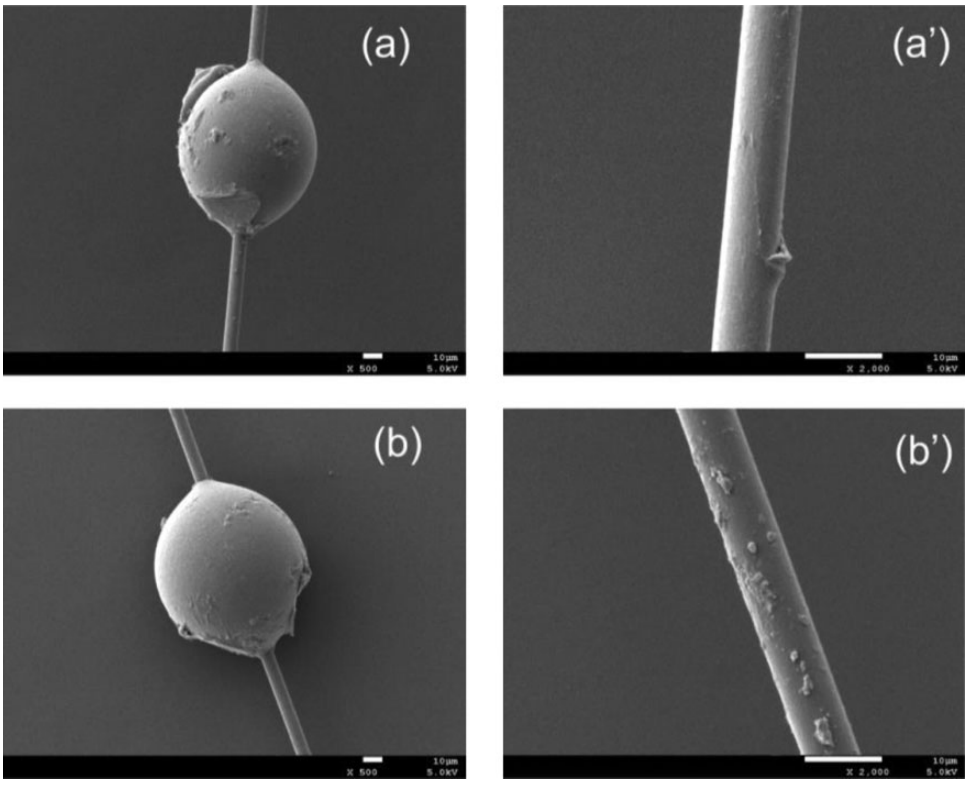

Figure 15. SEM images of CF/PPS microdroplets before debonding and surface of CF after debonding: (a, a′) samples with untreated PPS and (b, b′): samples with plasma-treated PPS. SEM: scanning electron microscopy; CF: carbon fiber; PPS: polyphenylene sulfide.

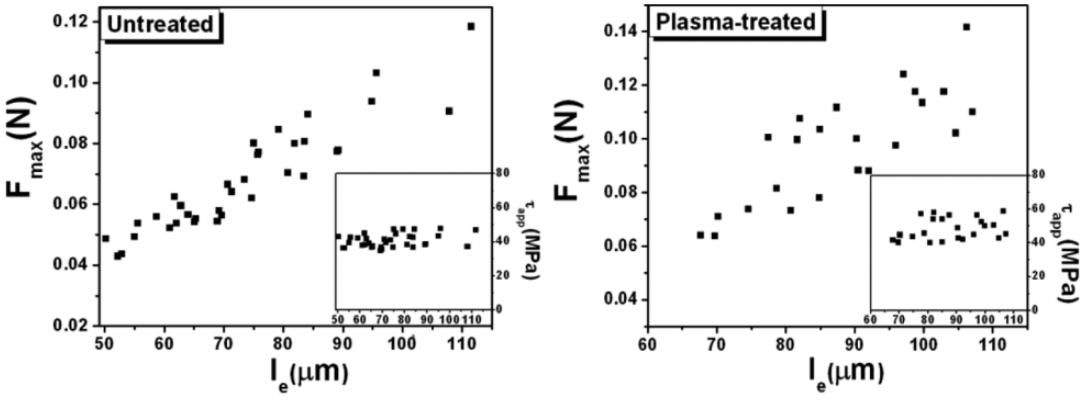

Figure 16. Microbond test results of CF/PPS composites with/without plasma treated PPS fiber. CF: carbon fiber; PPS: polyphenylene sulfide.

Table 7. Interfacial shear strength of PPS/CF samples with plasma-treated and untreated PPS fiber.

Samples	Not plasma treated	Plasma treated
τ_{app} (MPa, SD)	40.9 ± 3.9	47.9 ± 6.7

τ_{app}: interfacial shear strength; PPS: polyphenylene sulfide; CF: carbon fiber; SD: standard deviation.

3. Although plasma treatment grafts small amounts of polar groups on PPS fibers surface, the molecular structure of the resin under the surface remains unchanged. The treatment does not significantly change the overall crystal structure and the crystallinity of PPS resin. The matrix residues attached to the surface of CFs in the plasma-treated PPS fiber specimens are much more than those of pristine specimens. The τ_{app} was greatly enhanced (17.1%) by plasma treatment on the PPS fibers. The enhancement was due to the presence of the polarized PPS surface that could generate polar functional groups, such as sulfone(O=S=O), and sulfoxide(S=O), after plasma treatment. These groups can induce chemical reactions or generate hydrogen

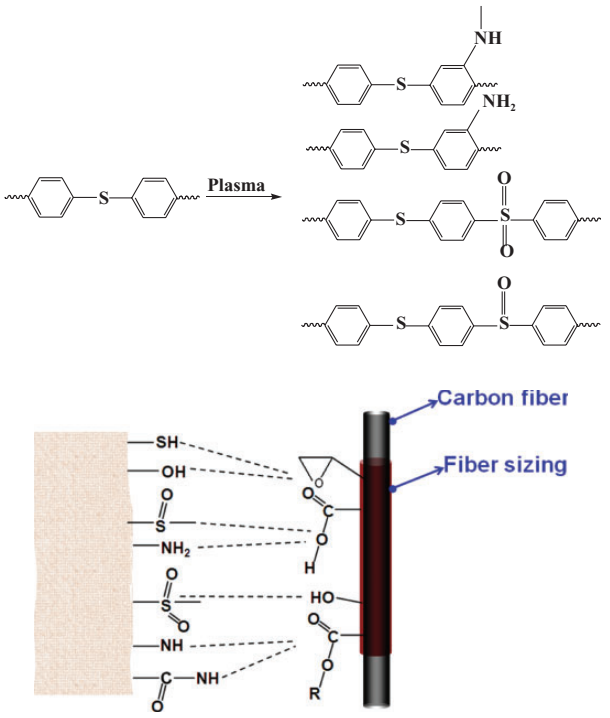

Figure 17. Schematic illustrations of interfacial reaction between CF and plasma-treated PPS fiber. CF: carbon fiber; PPS: polyphenylene sulfide.

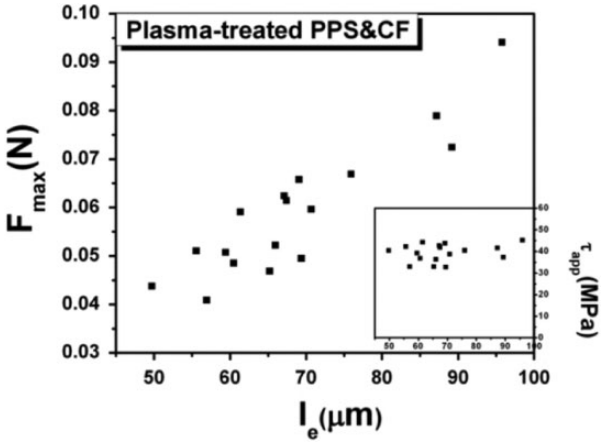

Figure 18. Microbond test results of CF/PPS composites with both PPS fiber and CF plasma treated. CF: carbon fiber; PPS: polyphenylene sulfide.

bond on CFs with some components of the sizing agents.

4. The τ_{app} of coprocessed specimens is lower than that of either untreated specimens or plasma-treated specimens. The main reason for the absence of synergistic effect is the removal of sizing agent, which was coated onto the surface of CFs by plasma etching.

The main factors in determining the adhesion between CFs and PPS matrix are the covalent bonds and micromechanical interlocking between the fiber and the matrix. For nonpolar polymer PPS, micromechanical interlocking is the primary factor that influences the interfacial strength of CF/PPS composite without plasma treatment. As a result of plasma treatment on PPS fibers, more covalent bonds form across the interface of CF/PPS composites than those on pristine specimens. Hence, interfacial adhesion of the composites can be enhanced by appropriate modifications.

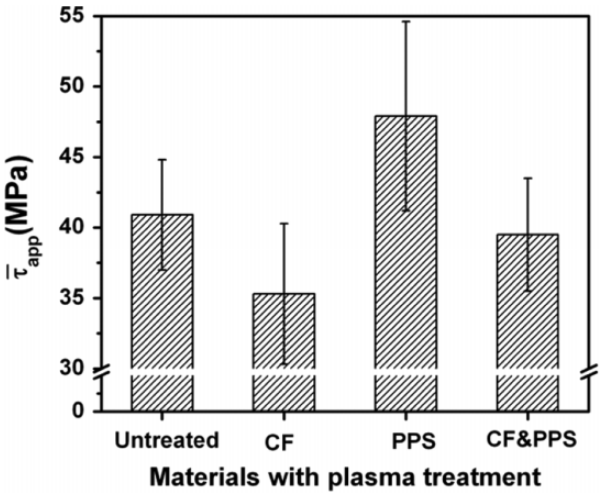

Figure 19. Comparison of interfacial shear strength of CF/PPS composites with different materials plasma treated. CF: carbon fiber; PPS: polyphenylene sulfide.

Table 8. Interfacial shear strength of PPS/CF samples with plasma-treated CF, PPS, and CF/PPS composite.

		Plasma treated		
Samples	Untreated	CF	PPS	CF/PPS cotreated
τ_{app} (MPa, SD)	40.9 ± 3.9	35.3 ± 5.0	47.9 ± 6.7	39.5 ± 4.0

τ_{app}: interfacial shear strength; PPS: polyphenylene sulfide; CF: carbon fiber; SD: standard deviation.

Funding

This research received no specific grant from any funding agency in the public, commercial, or not-for-profit sectors.

References

1. Yang JH, Xu T, Lu A, et al. Preparation and properties of poly (*p*-phenylene sulfide)/multiwall carbon nanotube composites obtained by melt compounding. *J Compos Sci Technol* 2009; **69**(2): 147–153.
2. Faria MCM, Appezzato FC, Costa ML, et al. The effect of the ocean water immersion and UV ageing on the dynamic mechanical properties of the PPS/glass fiber composites. *J Reinf Plast Compos* 2011; **30**(20): 1729–1737.

3. Lee BS, Chu BY, Chun L, et al. Effect of nylon66 addition on the mechanical properties and fracture morphology of poly(phenylene sulfide)/glass fiber composites. *J Polym Compos* 2003; **24**(1): 192–198.
4. Chen ZB, Liu XJ, Lü RG, et al. Mechanical and tribological properties of PA66/PPS blend. III. Reinforced with GF. *J Appl Polym Sci* 2006; **102**(1): 523–529.
5. Liu Z, Zhang SY, Huang GS, et al. Effects of polyarylene sulfide sulfone on the mechanical properties of glass fiber cloth-reinforced polyphenylene sulfide composites. *J High Perform Polym* 2015; **27**(2): 145–152.
6. Mark HF and Gaylord NG. *Encyclopedia of polymer science and technology*. New York: Wiley, 1969.
7. Lan MR. Tomorrow's plastic cars. ATSE focus CRC-ACS EP 01007 No. 113, July–August 2000.
8. Downing TD, Kumar R, Cross WM, et al. Determining the interphase thickness and properties in polymer matrix composites using phase imaging atomic force microscopy and nanoindentation. *J Adhes Sci Tech* 2000; **14**(14): 1801–1812.
9. Huang YD, Zhang ZQ, Tong Z, et al. Interfacial monitoring during the processing of carbon-fiber/PMR-15 polyimide composites. *J Mater Process Tech* 1993; **37**(1–4): 559–570.
10. Chan CM, Ko TM, Hiraoka H, et al. Polymer surface modification by plasmas and photons. *J Surf Sci Rep* 1996; **24**: 1–54.
11. Lu C, Chen P, Yu Q, et al. Interfacial adhesion of plasma treated carbon fiber/poly (phthalazinone ether sulfone ketone) composite. *J Appl Polym Sci* 2007; **106**: 1733–1741.
12. Hughes JDH. The carbon fibre/epoxy interface—a review. *J Compos Sci Tech* 1991; **41**(1): 13–45.
13. Zhang K, Zhang G, Liu BY, et al. Effect of aminatedpolyphenylene sulfide on the mechanical properties of short carbon fiber reinforced polyphenylene sulfide composite. *J Compos Sci Tech* 2014; **98**: 57–63.
14. Gonon FG, Fombarlet CM, Buda MJ, et al. Electrochemical treatment of pyrolytic carbon fiber electrodes. *J Anal Chem* 1981; **53**(9): 1386–1389.
15. Wu ZH, Charles U, Pittman JR, et al. Nitric acid oxidation of carbon fibers and the effects of subsequent treatment in refluxing aqueous NaOH. *J Carbon* 1995; **33**(5): 597–605.
16. Fitzer E and Weiss R. Effect of surface treatment and sizing of C-fibres on the mechanical properties of CFR thermosetting and thermoplastic polymers. *J Carbon* 1987; **25**(4): 455–467.
17. Yu B, Jiang ZY, Tang XZ, et al. Enhanced interphase between epoxy matrix and carbon fiber with carbon nanotube-modified silane coating. *J Compos Sci Tech* 2014; **99**: 131–140.
18. Li JQ, Huang YD, Xu ZW, et al. High-energy radiation technique treat on the surface of carbon fiber. *J Mater Chem Phys* 2005; **94**(2): 315–321.
19. Yao LR, Li M, Wu Q, et al. Comparison of sizing effect of T700 grade carbon fiber on interfacial properties of fiber/BMI and fiber/epoxy. *J Appl Surf Sci* 2012; **263**: 326–333.
20. Inoue K and Minami H. *Sizing agents for carbon fibers*. Patent 4904818, USA 1990.
21. Amornsakchai T and Psttarachindanuwong S. Surface grafting of polyethylene fiber for improved adhesion to acrylic resin. *J Reinf Plast Comp* 2010; **29**(1): 149–158.
22. Niu PF, Liu BY, Wei XM, et al. Study on mechanical properties and thermal stability of polypropylene/hemp fiber composites. *J Reinf Plast Comp* 2011; **30**(1): 36–44.
23. Iqbal HMS, Bhowmik S, and Benedictus R. Surface modification of high performance polymers by atmospheric pressure plasma and failure mechanism of adhesive bonded joints. *Int J Adhes* 2010; **30**(6): 418–424.
24. Yuan LY, Shyu SS and Lai JY. Plasma surface treatments on carbon fibers. II. Mechanical property and interfacial shear strength. *J Appl Polym Sci* 1991; **42**(9): 2525–2534.
25. Zheng ZW, Ren L, Feng WJ, et al. Surface characterization of polyethylene terephthalate films treated by ammonia low-temperature plasma. *J Appl Surf Sci* 2012; **258**(18): 7207–7212.
26. Xiong YL, Gu JY and Hu YC. Study on bonding performances of air plasma treated FRP. *J Mater Sci Forum* 2010; **658**: 236–239.
27. Kelly A and Tyson WR. Tensile properties of fibre-reinforced metals: copper/tungsten and copper/molybdenum. *J Mech Phys Sol* 1965; **13**(6): 329–350.
28. Mandell JF, Chen JH, and McGarry FJ. A microdebonding test for in situ assessment of fibre/matrix bond strength in composite materials. *Int J Adhes Adhes* 1980; **1**(1): 40–44.
29. Broutmari LJ. Measurement of the fiber-polymer matrix interfacial strength. *J Inter Compos* 1969; **452**: 27.
30. Miller B, Muri P and Rebenfeld L. A microbond method for determination of the shear strength of a fiber/resin interface. *J Compos Sci Technol* 1987; **28**(1): 17–32.
31. Zhou YX, Wang Y, Xia YM, et al. Tensile behavior of carbon fiber bundles at different strain rates. *J Mater Lett* 2010; **64**(3): 246–248.
32. Zhang SY, Huang GS, Wang X, et al. Effect of air plasma treatment on the mechanical properties of polyphenylene sulfide/glass fiber cloth composites. *J Reinf Plast Comp* 2013; **32**(11): 786–793.
33. Liu BY, Liu Z, Wang X, et al. Interfacial shear strength of carbon fiber reinforced polyphenylene sulfide measured by the microbond test. *J Polym Test* 2013; **32**(4): 724–730.
34. Zhandarov S and Mäder E. Characterization of fiber/matrix interface strength: applicability of different tests, approaches and parameters. *J Compos Sci Technol* 2005; **65**(1): 149–160.
35. Cwikel D, Zhao Q, Liu C, et al. Comparing contact angle measurements and surface tension assessments of solid surfaces. *Langmuir* 2010; **26**(19): 15289–15294.
36. Wu S. *Polymer interface and adhesion*. New York: Marcel of the C1s photo peak. Dekker, 1982.
37. Su M, Gu AJ, Liang GZ, et al. The effect of oxygen-plasma treatment on Kevlar fibers and the properties of Kevlar fibers/bismaleimide composites. *J Appl Surf Sci* 2011; **257**(8): 3158–3167.

38. Ehlers GFL, Fisch KR, and Powell WR. Thermal degradation of polymers with phenylene units in the chain. II. Sulfur-containing polyarylenes. *J Polym Sci A-1: Polym Chem* 1969; **7**(10): 2955–2967.
39. Napolitano R, Pirozzi B, and Iannelli P. Influence of the temperature on the crystal structure of poly(p-phenylene sulfide): a study by X-ray measurements and molecular mechanics. *J Macromol Theor Simul* 2001; **10**(9): 827–832.
40. Seo KH, Park LS and Baek JB. Thermal behaviour of poly (phenylene sulfide) and its derivatives. *J Polymer* 1993; **34**(12): 2524–2547.